Output-coupling semiconductor saturable absorber mirror

G. J. Spühler, S. Reffert, and M. Haiml
Ultrafast Laser Physics, Institute of Quantum Electronics, Swiss Federal Institute of Technology, ETH Hönggerberg-HPT CH-8093 Zürich, Switzerland

M. Moser
Centre Suisse d'Electronique et de Microtechnique–Zürich, Badenerstrasse 569 CH-8048 Zürich, Switzerland

U. Keller[a)]
Ultrafast Laser Physics, Institute of Quantum Electronics, Swiss Federal Institute of Technology, ETH Hönggerberg-HPT CH-8093 Zürich, Switzerland

(Received 23 October 2000; accepted for publication 7 March 2001)

We present a semiconductor saturable absorber mirror (SESAM), which also acts as an output coupler at the same time. The influence of the output coupler transmission onto the absorber parameters is investigated theoretically, as well as experimentally. A passively *Q*-switched Nd:YVO_4 microchip laser is built using such a nonlinear output coupler, yielding clean pulses of 143 ps duration, 48 nJ energy, and 572 W peak power. This result is compared with the traditional approach, where the SESAM is not used as an output coupler. © *2001 American Institute of Physics.* [DOI: 10.1063/1.1370122]

Semiconductor saturable absorber mirrors (SESAMs)[1,2] are well established as a useful device for passive mode locking and *Q* switching of many kinds of solid-state lasers.[3] The main reason for this device's utility is that both the linear and nonlinear optical properties can be engineered over a wide range, allowing for more freedom in the specific laser cavity design. The main absorber parameter such as operation wavelength λ, modulation depth ΔR, saturation fluence F_{sat}, and absorber life time τ_A can be custom designed for stable cw mode locking or *Q* switching. Initially, semiconductor saturable absorber mirrors were used in coupled cavities,[4] because they introduced too much loss inside solid-state lasers with small gain cross sections (i.e., 10^{-19} cm^2 and smaller). Two years later, in 1992, this work resulted in another type of intracavity saturable absorber mirror, the antiresonant Fabry–Perot saturable absorber (A-FPSA),[1] where the absorber was integrated inside a Fabry–Perot structure of which the bottom reflector was a high reflector (i.e., approximately 100%). The Fabry–Perot was operated at antiresonance to obtain broad bandwidth and low loss. The A-FPSA mirror was mainly based on semiconductor Bragg mirror and absorber layers and therefore allowed for a large variation of the absorber. The result was a much better understanding of the absorber and laser design necessary to obtain stable passive mode locking or *Q* switching of many different solid-state lasers. In 1995[5] it was further realized that the intracavity saturable absorber can be integrated in a more general mirror structure that allows for both saturable absorption and negative dispersion control, which is now generally referred to as a SESAM.[2] In a general sense we then can reduce the design problem of a SESAM to the analysis of multilayered interference filters for a given desired nonlinear reflectivity response in both the amplitude and phase. The A-FPSA,[1] the saturable Bragg reflector,[6] and the dispersive saturable absorber mirror[7] are then special examples of SESAM designs.

With a few exceptions,[8] the SESAM is mostly used as an end mirror of a standing-wave cavity, which can lead to a higher complexity of the laser setup. This was observed for example in passively *Q*-switched microchip laser[9,10] and passively mode-locked miniature lasers[11–13] where a short laser crystal defines a monolithic cavity. The SESAM attached to the laser crystal then formed one end mirror of this laser cavity. As the laser cannot be pumped through the SESAM, the laser output needs to be separated from the pump by a dichroic mirror. These examples suggest that there is need for a device which combines the nonlinear properties of the SESAM with an output coupler. This has been demonstrated before for a passively mode-locked fiber laser.[14]

In this letter we investigated possible limitations of combining a SESAM with an output coupler (SESAMOC). We compare the nonlinear reflectivity response and the performance with a passively *Q*-switched Nd:YVO_4 microchip laser using either a classic SESAM as a high reflector or a SESAM as output coupler. The difference between the two SESAM designs is only in the bottom Bragg mirror structure as shown in Fig. 1. The SESAM consists of an AlAs/GaAs bottom Bragg mirror metalorganic chemical vapor deposition (MOCVD) grown on an undoped GaAs substrate and a saturable absorber formed by five groups of 8.7 nm thick $In_{0.25}Ga_{0.75}As$/GaAs multiquantum well structures placed at the peak of the standing wave pattern at 1.064 μm within a transparent GaAs spacer layer. We can then change this highly reflective SESAM device to a SESAMOC by simply reducing the reflectivity of the lower AlAs/GaAs Bragg mirror. In the first case the reflecting Bragg mirror has a reflectivity close to 100% and consists of 22 AlAs/GaAs quarter wave layer pairs. In the second case we use only seven quarter wave pairs resulting in a bottom reflectivity of 90% to optimize the pulse energy of a passively *Q*-switched microchip laser. High pulse energy requires an output coupling transmission T_{out} of the same order as ΔR.[10] Because the two devices have identical absorber structures and nearly the

a)Electronic mail: keller@iqe.phys.ethz.ch

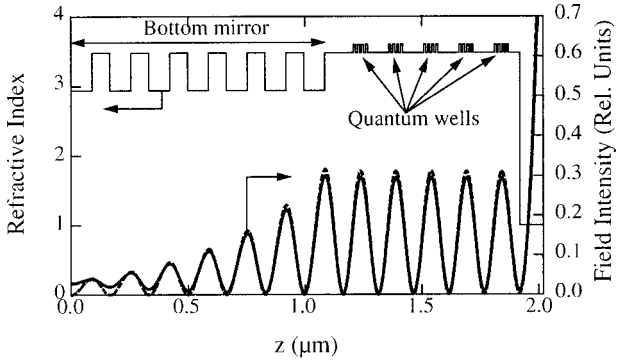

FIG. 1. SESAM structure shown with the refractive index profile of the different layers and standing wave intensity pattern at $\lambda=1.064$ μm. The thick solid line corresponds to the standing wave in the SESAM with a 100% bottom reflector (of which only seven Bragg pairs are shown) and the dashed line corresponds to the standing wave pattern in the SESAM output coupler.

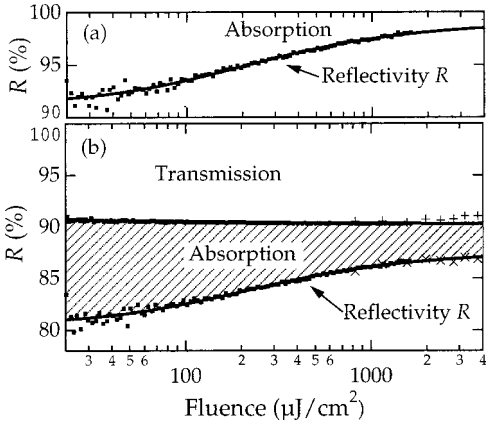

FIG. 2. Nonlinear reflectivity (and transmission) vs incident pulse fluence (dots) and theoretical fit (solid curves) (a) for the SESAM with 100% bottom reflector and (b) for the SESAM with a 10% output coupler. Dots: measured with a 7 ps Nd:YVO_4 laser at 1064 nm; Crosses: measured with a high power 7 ps Yb:YAG laser at 1030 nm and rescaled to take into account the wavelengths dependent transmission and reflectivity of the lower Bragg mirror.

same intensity in the absorber layers (see standing wave pattern in Fig. 1) they also have very similar absorber properties ΔR, F_{sat}, and τ_A. This can be stated for any classic SESAM structure, when we look at the scaling factor for the peak intensity of the standing wave inside the absorber layers compared to the intensity outside of the SESAM [Eq. (13) of Ref. 15]. Even for $T_{\mathrm{out}}=15\%$ and ΔR of 15%, the intensity in the absorber layers changes by less than 5%. This implies that we can change the number of Bragg pairs and thus T_{out} of a SESAM for a given absorber structure without substantially changing the absorber parameters. In addition, for mode-locked solid-state lasers, ΔR and T_{out} are usually even smaller than for *Q*-switched lasers (typically $\Delta R\approx 1\%-2\%$ and $T_{\mathrm{out}}\leqslant 5\%$).

There are a number of additional complicating issues however for a SESAMOC. The device has to be grown on a nonabsorbing substrate, which in our case was an undoped GaAs wafer, polished on both sides, and the back side of the wafer has to be antireflection (AR) coated in order to avoid residual back reflections and thus additional etalon effects, which could degrade the nonlinear response. These residual losses in the substrate can reach a few percent. However, it should be noted that these are extracavity losses and do not affect the internal laser dynamics. As an alternative, the substrate could be etched away. This would be required in wavelength regimes where no transparent substrates are available or if the nonlinear losses in the substrate become high.

The SESAM was grown with MOCVD at normal growth temperatures which typically results in an absorber recovery time of several hundred picoseconds. The devices are characterized in a saturation measurement setup, where we determine the nonlinear reflectivity and transmission as a function of the pulse fluence incident on the device. For these characterizations we used a passively mode-locked Nd:YVO_4 laser with pulses of 7 ps duration laser. The saturation measurement of the SESAM and the SESAMOC are shown in Fig. 2 together with the theoretical fits. For the standard SESAM, we measure $\Delta R=8\%$, $F_{\mathrm{sat}}=111$ μJ/cm^2, and nonsaturable losses of $\Delta R_{\mathrm{ns}}=0.9\%$. The measured saturation fluence for the SESAMOC ($F_{\mathrm{sat}}=115$ μJ/cm^2) agrees very well with the classic device, and also the modulation depth ($\Delta R=7.1\%$) is similar, as expected from the standing wave pattern shown in Fig. 1. We fitted the nonlinear transmission with the same function as the nonlinear reflectivity. However, the change in transmission is too small (i.e., smaller than the absolute accuracy of the measurement) to get a reliable value for the saturation fluence. The linear losses of $\approx$2.7% not originating from the output coupling are contributed mainly to the residual losses in the undoped GaAs substrate and the imperfect AR coating. But these losses are extracavity losses, which do not affect the laser dynamics, but of course will affect the available output power. The measured saturated transmission of 9.8% agrees well with the designed 10.1%. It is important to note that with significantly shorter pulses nonlinear losses due to two photon absorption in the substrate will increase. For example numerical simulations show that the losses in the 450 μm thick GaAs substrate can reach 10% for pulses of 1 ps duration and 1.5 mJ/cm^2 incident on the device (assuming $T_{\mathrm{out}}=10\%$).

We then compared the two devices in a passively *Q*-switched microchip laser. The laser, similar to the one presented in Ref. 9, consists of a *a*-cut 200 μm thin AR coated 3 at. %-doped Nd:YVO_4 gain element sandwiched between the SESAM and the output coupler or between the SESAMOC and a high reflector, respectively (Fig. 3). The laser is pumped by an 808 nm single emitter diode of 200 μm stripe size focused to a spot radius of 78 μm$\times$23 μm in the laser crystal. With the classic SESAM, we use a dielectric output coupler of 8.7% transmission at 1064 nm and

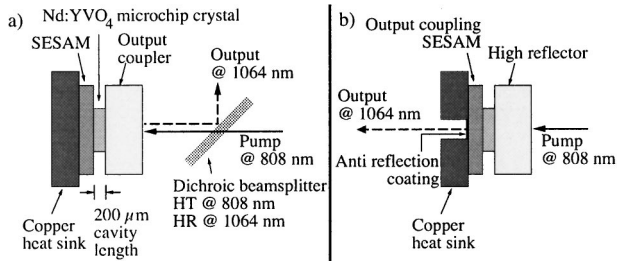

FIG. 3. Cavity setup of the microchip laser containing (a) the high reflecting SESAM and (b) the output coupling SESAM.

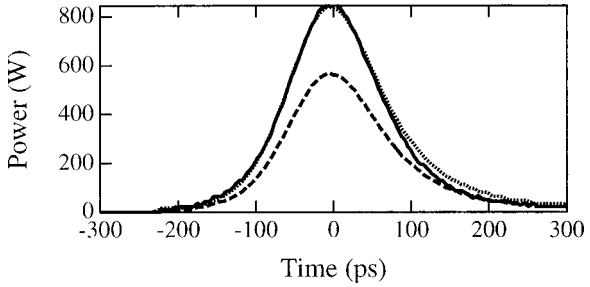

FIG. 4. Typical *Q*-switched pulse of the microchip laser: Solid: SESAM, dashed: SESAM with output coupling, dotted: dashed curve scaled to compare the pulse shapes.

85% at 808 nm. With the SESAMOC (saturated T_{out} 9.8%, Fig. 2), we pump through a high reflector with a transmission of 99.5% for the pump wavelength. For comparison the difference in the pump transmission has been compensated for by the amount of incident pump power. In Fig. 4 typical *Q*-switched pulses of the microchip lasers with the two different setups are shown with a pulse duration of 143 ps and an energy of 70 nJ (SESAM) and 48 nJ (SESAMOC), respectively. The pump power on the microchip was 160 mW and the average output power was 13.9 mW with a pulse repetition rate of 198 kHz (SESAM) and 7.7 mW with 160 kHz (SESAMOC). This corresponds to an absorber saturation level of ≈24 times the saturation fluence. It can be seen that the quality of the pulses (shape and duration) is indeed comparable. However, we typically get about 30%–50% less average power and pulse energy when we couple out through the SESAM. This is much less than we would have expected from our saturation measurements (Fig. 2) which give a residual loss of only ≈3% for a fully saturated absorber at 35 times the saturation fluence (4 mJ/cm^2 in Fig. 2). Given that we cannot have such high nonlinear losses in the GaAs substrate with pulses that are even much longer than the laser pulses we have used to characterize the nonlinear response, we must conclude that the different thermal situation in the two microchip lasers is the reason for the decrease in performance. In order to be able to couple out through the SESAMOC we need a hole in the heat sink (here about 5 mm diameter) which the SESAMOC is soldered onto [see Fig. 3(b)]. This hole is located directly behind the pump spot and affects the heat flow substantially. Additionally, the dielectric AR coating on the back of the substrate (i.e., between the substrate and the solder layer) acts as a bottleneck for the heat transfer. Therefore, the heat flux and the temperature gradients are changed significantly (value and direction) if we use the SESAMOC. As the thermal lens is the stabilizing effect for the flat-flat cavity,[16,17] the laser mode size depends strongly on the thermal conditions. According to Ref. 10 the pulse energy of a passively *Q*-switched microchip laser is directly proportional to the mode area in the laser. Then the pulse energy difference of our two setups can be explained by the different thermal conditions, which leads to different laser mode sizes and therefore lower average output power due to a higher threshold of the laser. We would expect that the average pulse energy can be recovered to a great extent with pump spot size optimizations, smaller holes in the heat sink, etc. However, the pulse duration depends only on the modulation depth of the saturable absorber (and the cavity length)[10] and is therefore not affected by the different mode sizes. In Fig. 4 we have normalized the pulse coupled out through the SESAMOC (dashed) to the same peak power as the pulse of the standard setup (×1.47, dotted), and indeed the pulse duration and shape agree very well.

It is important to note that the microchip laser is particularly sensitive to heat sinking because we only obtain a stable laser cavity due to the thermal lens. In contrast, the high-repetition rate miniature laser[11–13] does not have a flat-flat cavity but one curved side which forms a stable laser cavity also without the thermal lens of the pump laser. Thus, we would expect only an output power degradation of a few percent, consistent with the nonlinear reflectivity measurements when coupling out through the SESAMOC. Of course the saturable absorber parameters would have to be adjusted to prevent *Q*-switched mode locking.[18]

In conclusion, we have presented a modification of the standard SESAM, which allows for use as an output coupler. We have shown that this modification does not affect the basic absorber parameters and that the concept of the output coupling SESAMs can be applied for passively *Q* switched as well as for passively mode-locked laser in the picosecond regime. We have characterized the performance of an output coupling SESAM in a saturation measurement and in a passively *Q*-switched microchip laser. The saturation measurement shows that the output coupling equivalent of the SESAM has indeed comparable absorber parameters.

The authors would like to thank J. Aus der Au and F. Brunner for helpful discussions and Time-Bandwidth Products Inc. for the picosecond Nd:YVO_4 laser (Model Picolo-TC) which was used for the saturation measurements

[1] U. Keller, D. A. B. Miller, G. D. Boyd, T. H. Chiu, J. F. Ferguson, and M. T. Asom, Opt. Lett. **17**, 505 (1992).
[2] U. Heller, K. J. Weingarten, F. X. Kärtner, D. Kopf, B. Braun, I. D. Jung, R. Fluck, C. Hönninger, N. Matuschek, and J. Aus der Au, IEEE J. Sel. Top. Quantum Electron. **2**, 435 (1996).
[3] U. Keller, in *Nonlinear Optics in Semiconductors*, edited by E. Garmire and A. Kost (Academic, Boston, MA, 1999), Vol. 58, p. 211.
[4] U. Keller, W. H. Knox, and H. Roskos, Opt. Lett. **15**, 1377 (1990).
[5] U. Keller and D. Kopf, European Patent Nr. EP 0 826 164 B1, priority date 19 May 1995.
[6] S. Tsuda, W. H. Knox, E. A. d Souza, W. Y. Jan, and J. E. Cunningham, Opt. Lett. **20**, 1406 (1995).
[7] D. Kopf, G. Zhang, R. Fluck, M. Moser, and U. Keller, Opt. Lett. **21**, 486 (1996).
[8] B. Braun and U. Keller, Opt. Lett. **20**, 1020 (1995).
[9] B. Braun, F. X. Kärtner, M. Moser, G. Zhang, and U. Keller, Opt. Lett. **22**, 381 (1997).
[10] G. J. Spühler, R. Paschotta, R. Fluck, B. Braun, M. Moser, G. Zhang, E. Gini, and U. Keller, J. Opt. Soc. Am. B **16**, 376 (1999).
[11] L. Krainer, R. Paschotta, G. J. Spühler, M. Moser, and U. Keller, Electron. Lett. **35**, 1160 (1999).
[12] L. Krainer, R. Paschotta, M. Moser, and U. Keller, Appl. Phys. Lett. **77**, 2104 (2000).
[13] L. Krainer, R. Paschotta, M. Moser, and U. Keller, Electron. Lett. **36**, 1846 (2000).
[14] R. C. Sharp, D. E. Spock, N. Pan, and J. Elliot, Opt. Lett. **21**, 881 (1996).
[15] L. R. Brovelli, U. Keller, and T. H. Chiu, J. Opt. Soc. Am. B **12**, 311 (1995).
[16] J. J. Zayhowski and A. Mooradian, Opt. Lett. **14**, 24 (1989).
[17] J. J. Zayhowski, C. D. Ill, C. Cook, and J. L. Daneu, OSA TOPS **26**, 178 (1999).
[18] C. Hönninger, R. Paschotta, F. Morier-Genoud, M. Moser, and U. Keller, J. Opt. Soc. Am. B **16**, 46 (1999).